

56. *Micro-structure of the Seismic Sequence Related to a Moderate Earthquake.*

By Masakazu OHTAKE,

Earthquake Research Institute.

(Read June 23, 1970.—Received September 30, 1970.)

Summary

Micro-seismicity was investigated concerning the seismic sequence related to a moderate earthquake which occurred on April 9 of 1970 in the swarm area of the Matsushiro earthquakes. Though the area of the aftershock activity was as small as 18 km², the following peculiar features were found by a precise analysis. (1) The foreshock and the larger aftershocks seem to be arranged on a inclined plate, whose length and width are 10 km and 2 km, respectively. (2) Most of the smaller aftershocks cluster by the upper side of this plate. (3) The main shock is located on the deeper end of the plate, and the aftershock activity is rather weak around it.

Regarding the push-pull distribution of the main event, the fracture accompanying the main shock is supposed to have run upwards for ten kilometers along the plane of the larger aftershocks. The dislocation may be a left-lateral strike slip.

Another interesting characteristic is the independent behavior of the active groups in the swarm area. The present event, which occurred in one of the southwestern active groups, never excited nor stilled the ordinary seismic activity of the other groups. This fact would be reflecting the mosaic structure of the medium, and would explain the curious lacking of larger shocks through the Matsushiro earthquake swarm. The continuous observation with broad dynamic range was essential for this study.

1. Introduction.

The detailed studies on the time and space distribution of fore- and after-shocks will give useful information on the process of the fracturing accompanying the main shock. The networks for microearthquakes are suitable to make such investigations concerning the smaller earthquakes, whose aftershocks would be missed except for some larger ones by the seismographs with low magnification. Main shocks and larger aftershocks, however, are sometimes scaled out at the stations for microearthquakes because of their high sensitivity, and so it is rather difficult to treat

consistently the larger and smaller ones. To avoid such difficulties, we installed the instruments of low magnification with the same frequency response at the Hokushin Observatory of Microearthquakes and Crustal Deformation. Supplemented with the data from these low magnification channels, a detailed description is made on a moderate earthquake, which took place near Matsushiro on April 9, 1970, and on some peculiar characteristics in the local seismicity before and after it.

2. Data.

Used data are the smoked paper records of the Hokushin Observatory and its satellite stations, where are maintained the high sensitivity instruments with three components. The locations of the stations are shown on Fig. 1, with the epicenter of the main shock. Second signals are marked on the records, whose paper speed is 4 mm/sec, and we can safely read the commencement times at an accuracy of 0.01 sec if the onset of the waves is sharp enough. Time difference of the crystal clocks is checked every hour, excepting midnight, with the hour signals of NHK broadcast. The natural period of the seismographs is 1.0 sec and the overall velocity sensitivity is actually constant within the fre-

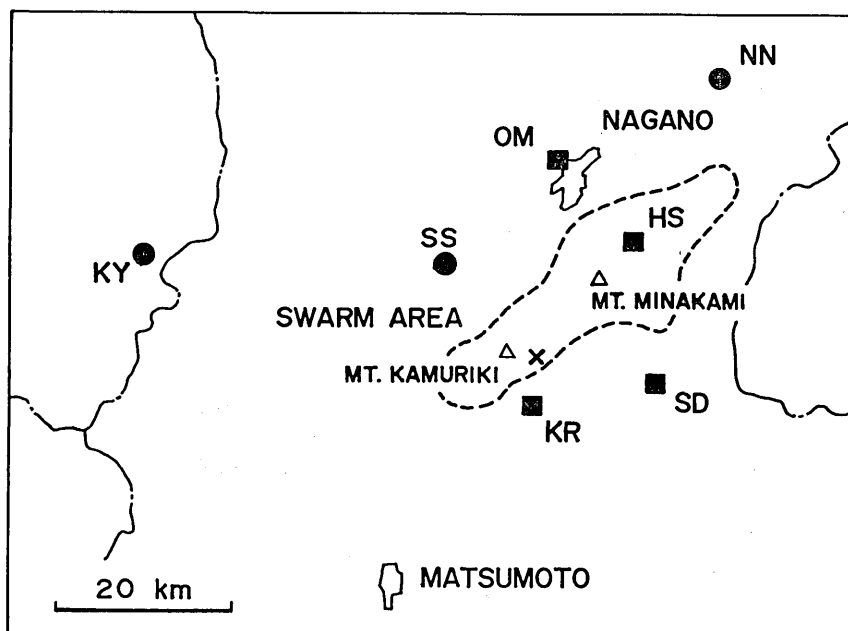


Fig. 1. The epicenter of the main shock (\times), and the observation stations of the Hokushin Observatory (■: smoked-paper type, ●: optical type). The names of the stations are shown with the local codes which are listed on Table 1.

Table 1. The sensitivity and magnification of the observation stations

Name of the station	Local code	Sensitivity or magnification	Recording type
Ohmine	OM	0.51 K cm/kine 40 4.0 0.4	Smoked paper
Hoshina	HS	2.8 K	
Sanada	SD	0.19 K	
Kami-muroga	KR	1.2 K	
Nakano	NN	10 K	Optical (HES 1-0.2)
Shinshu-shinmachi	SS	10 K	
Kuroyon	KY	50 K	

quency range between 1.5 and 25 Hz. The sensitivity at each station is listed on Table 1.

Records of lower magnifications are available only at Ohmine (OM), which is the key station of the Hokushin Observatory. They are composed of three channels with the same frequency response and the different sensitivities. The magnification of the first channel is settled at -22 db of the high sensitivity instruments, and that of the second and the third channels is lower by 20 db one by one. At Ohmine we can cover a wide dynamic range of 80 db, *i.e.* 4.0 in the magnitude range by the combination of the high and the low magnification instruments. For the present case, all shocks with a magnitude larger than 1.2 are clearly recorded at Ohmine without saturation or under exposure.

3. The main shock.

On April 9 of 1970, the main shock took place in the southwestern part of the area of the Matsushiro earthquake swarm (Fig. 1). Its

Table 2. The parameters of the earthquake which occurred near Matsushiro at 01h44m on April 9 of 1970 (JST)

	Hokushin	JMA	USC&GS
Origin time	44 ^m 00. ^s 83	43 ^m 59. ^s 1	44 ^m 01. ^s 04
Epicenter $\left\{ \begin{array}{l} \lambda \\ \varphi \end{array} \right.$	138°09'.0E 36°28'.3N	138°06'E 36°26'N	138°.159E 36°.459N
Depth	14.3 km	0	8 km
Magnitude	5.2	5.0	*4.3

* body wave magnitude.

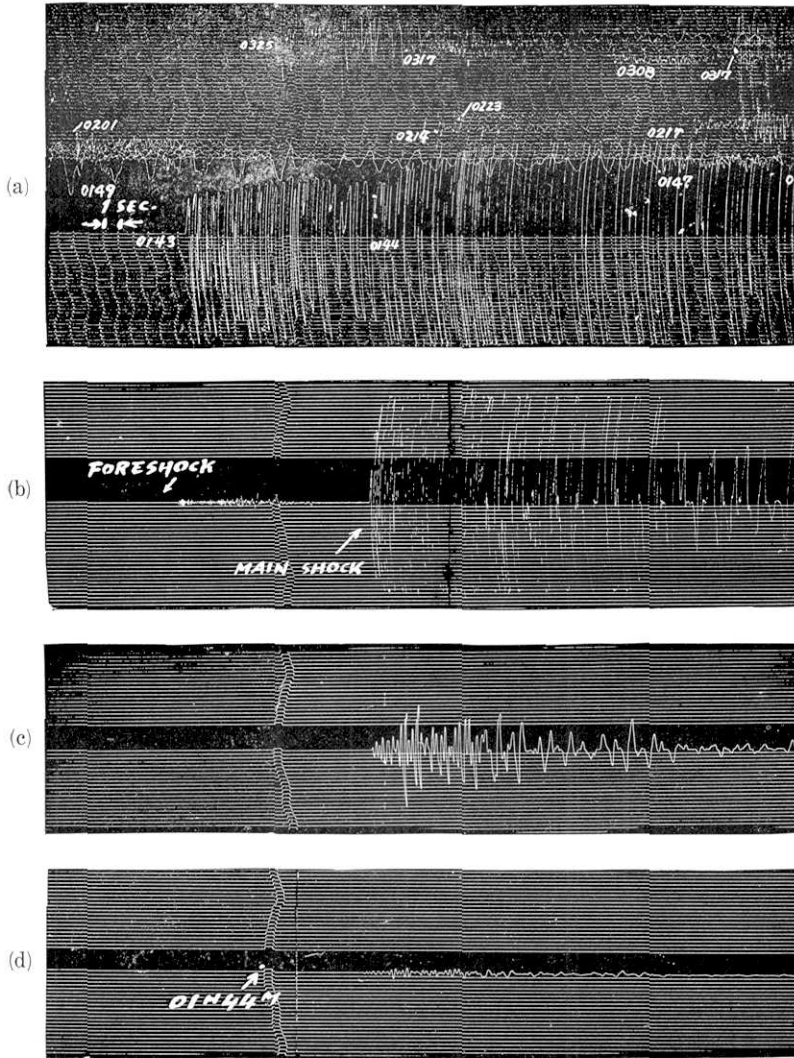


Fig. 2. The traces of the main shock (vertical component) recorded at Ohmine with the instrument of high sensitivity (a), and those of lower sensitivity ((b)~(d)).

magnitude was 5.0 by Japan Meteorological Agency. Such a remarkable shock had not been observed since April 4 of 1968. The calculated parameters of this earthquake are listed on Table 2, including the values by JMA and USC&GS.

The traces of this shock at Ohmine are reproduced in Fig. 2. The feature of the main shock is somewhat different from that of typical aftershocks in our frequency range. The amplitude of the first motion is very small and is only 1/30 of the maximum amplitude (vertical component). The ground vibration seems to be gradually built up till its

climax. The onset of the after-shocks is, on the contrary, very sharp and the amplitude ratio between the first motion and the maximum one is $1/2 \sim 1/5$ in most cases. This discrepancy of the amplitude ratio is not explained by the difference of the focal mechanism, because the same tendency is found even at the other stations.

The compression axis of the main shock lies almost horizontal and the direction of it is estimated to be $N55^\circ \pm 3^\circ W$ from the push-pull distribution of the first motions shown on Fig. 3. This solution does not coincide with that of the ordinary Matsushiro earthquakes investigated by Ichikawa (1969).

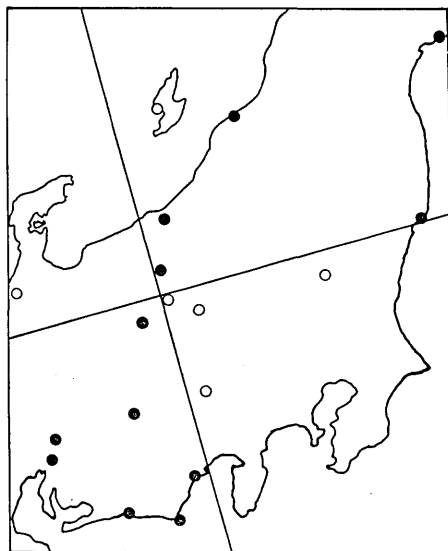


Fig. 3. The push-pull distribution of the initial motions of the main shock. Solid and open circles indicate up and down movement of the first motions, respectively.

4. Computing procedure of the hypocenters.

The origin time of the shocks is fixed by the data at Ohmine following the formula:

$$O.T. = t_p - \{(S-P) - 0.40\} / 0.67,$$

where t_p and $S-P$ indicate the arrival time of P and the $S-P$ interval, respectively. A constant substituted from $S-P$ is due to a systematic delay of S waves at Ohmine. The apparent Poisson's ratio of the medium is calculated to be 0.22 from the value of 0.67 in the formula. The data and the discussions of these values will appear in another paper (in preparation). Referred to this origin time the hypocenter is computed from the travel times of P at the three stations; Ohmine (OM), Sanada (SD), and Kami-muroga (KR). Hypocentral distances are given as a function of travel times and focal depths for each station. The computation is iterated till the depth converges within one kilometer. The fourth station, Hoshina (HS) is used only to check the computed coordinates. From the data of explosion seismic observations, Asano *et al.* (1969) derived a fine structure model of the P wave velocities of the upper crust around Matsushiro. Based on their results we adopted

DEPTH (km)	V _p (km/sec)		
	OM	SD	KR
0.0 -	2.1	2.4	3.5
0.5 -		4.4	
2.5 -	4.0		
4.5 -		6.0	6.0
	6.0		
18.5 -	6.8	6.8	6.8

Fig. 4. The crustal structures which are used to compute the travel times.

different velocity structures for each station (Fig. 4).

As our present interest is centered upon finding a micro-structure of the focal distribution, only those three stations are used as a rule, in order to avoid systematic discrepancy caused by the difference in station sets. The main shock was unfortunately disturbed by a foreshock just before it, and the data of the farther optical stations, are also used. The hypocenter of the main shock, however, is referred to the other ones by the following procedure. We pick up a "standard" aftershock, of which hypocenter is accurately determined close to the main shock with the three stations; OM, SD and KR. A small difference in hypocentral distances of the two shocks, Δr , is connected with that in travel times, Δt , by the relation:

$$\Delta r = v \cdot \Delta t,$$

where v is the wave velocity of the medium around those shocks. Measuring the hypocentral distance of the "standard" aftershock geometrically, we can estimate the "referred" hypocentral distance of the main shock at the stations where the arrival times of the both shocks are available. These "referred" values are also used to calculate the hypocenter of the main shock. The focus of the main event would be successfully referred to those of the aftershocks by this treatment, although the accuracy may be a little worse.

Time accuracy of readings is 0.01 sec for P times and 0.1 sec for S - P intervals. Mutual locations of the shocks, therefore, would be relied on within 0.5 km for epicenters and 1.0 km for the depths.

5. Spatial distribution of the aftershocks.

On Fig. 5 (a) plotted are the epicenters of all the earthquakes located near the main shock in the thirty days from April 9 to May 9.

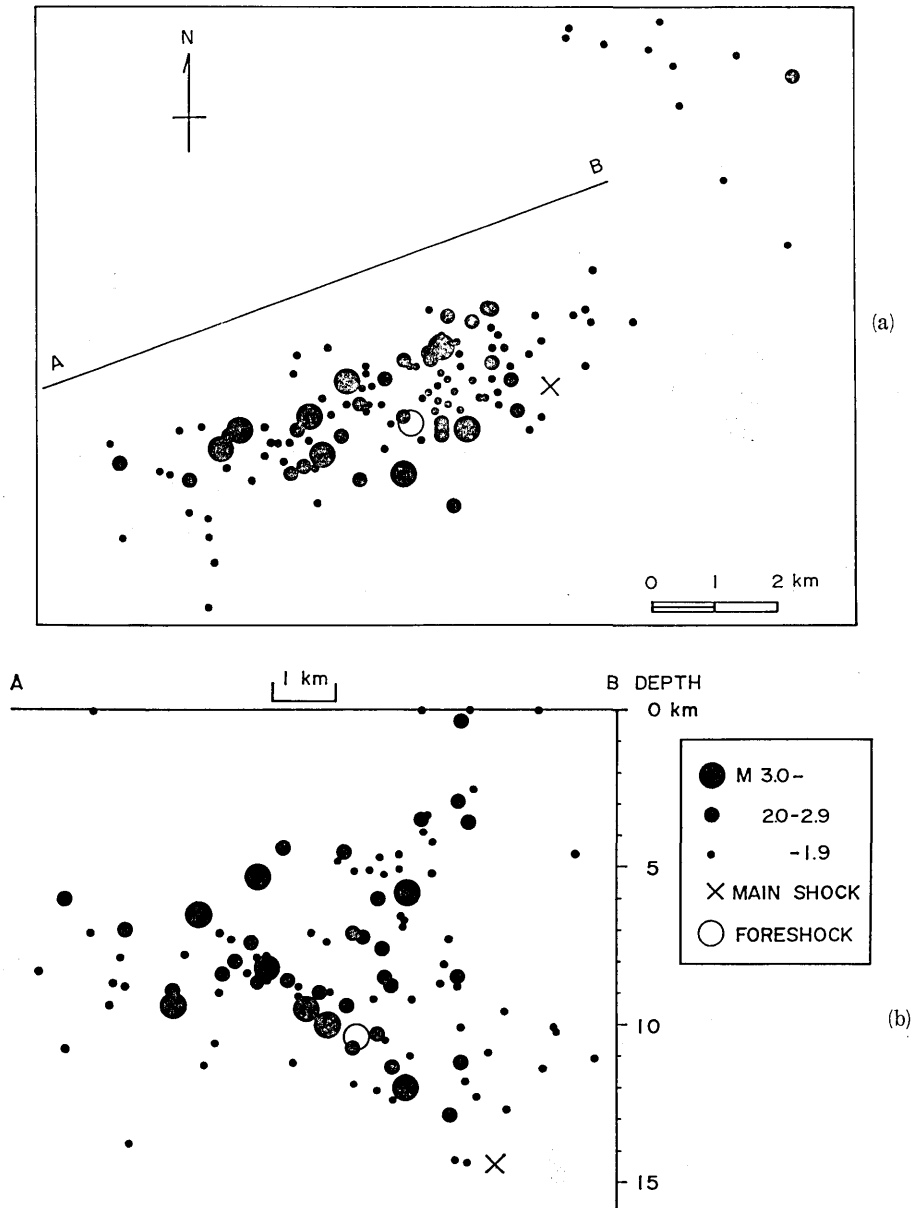


Fig. 5. (a) The epicentral distribution of the earthquakes which occurred within thirty days following the main shock. (b) The section map of the hypocentral distribution projected on a vertical plane trending $N70^{\circ}E$ (A-B).

Table 3. The area and the volume of the aftershock region and the corresponding values expected from the empirical relations

	Measured	Expected
Area	18 km ²	12 km ²
Volume	150 km ³	330 km ³

The active region of the aftershocks is clearly distinguished from the other ordinary activities of the Matsushiro earthquakes. The aftershocks are distributed almost within a rectangle of 9 km×2 km, placing the main shock near the eastern end of it. The longer axis of the distribution almost coincides with one of the nodal lines of the main shock. Fig. 5 (b) is the section map projected on a vertical plane trending N70°E. The larger aftershocks show a planer arrangement. This seismic plane has a strike of N20°W and a dip of 60° to the eastern side. This feature is never explained by the errors in *S-P* readings at Ohmine, because they would result in an inverse arrangement, *i.e.* the westwards inclination. Errors in *t_p* times are negligible. Most of the smaller aftershocks cluster by the upper (eastern) side of the plane. The aftershocks shallower than 9 km, however, do not show such a systematic arrangement. The focus of the main shock is located on the deepest end of the seismic plane; all the other shocks are shallower. Aftershock activity seems to be rather weak near the main shock. The area and the volume of the aftershock region is compared on Table 3 with the expected values from the statistical relations for larger earthquakes:

$$\log A = 1.02M_0 - 4.0, \quad (6 \leq M_0 < 8 \frac{1}{2}),$$

by Utsu and Seki (1955), and

$$\log V = 1.06M_0 - 2.78, \quad (6 \leq M_0 < 8 \frac{1}{2}),$$

by Iida (1963), where *A* and *V* are the active area (km²) and volume (km³) of the aftershocks, and *M₀* is the magnitude of the main shock, respectively. These empirical relations seem to be valid even in our case, though the present main shock is a little smaller than those investigated by the above authors.

6. Time series of the aftershocks.

On the next day of the main shock, 1,087 aftershocks were recorded at Kami-muroga, the nearest station from the foci. Daily number of the shocks, *n*, decreased following the power function:

$$n = n_1 \cdot t^{-h},$$

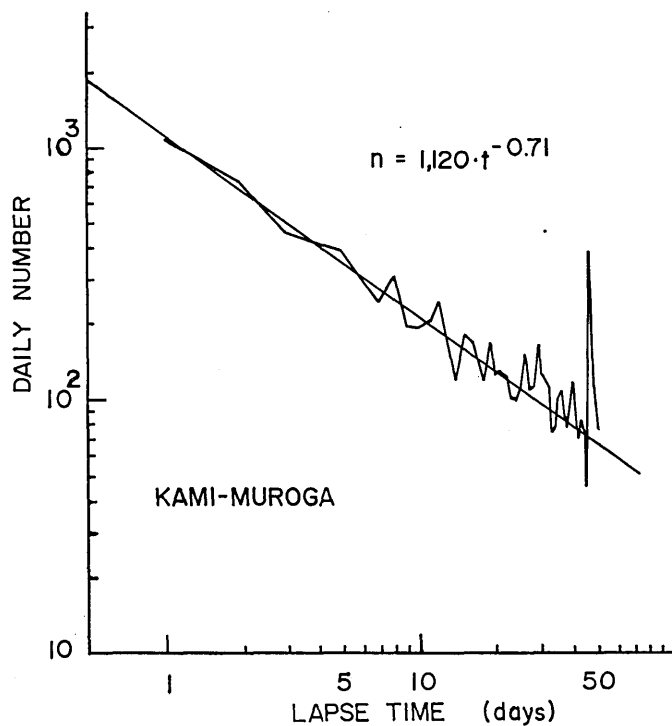


Fig. 6. The decaying feature of the frequency of the aftershocks against the lapse time.

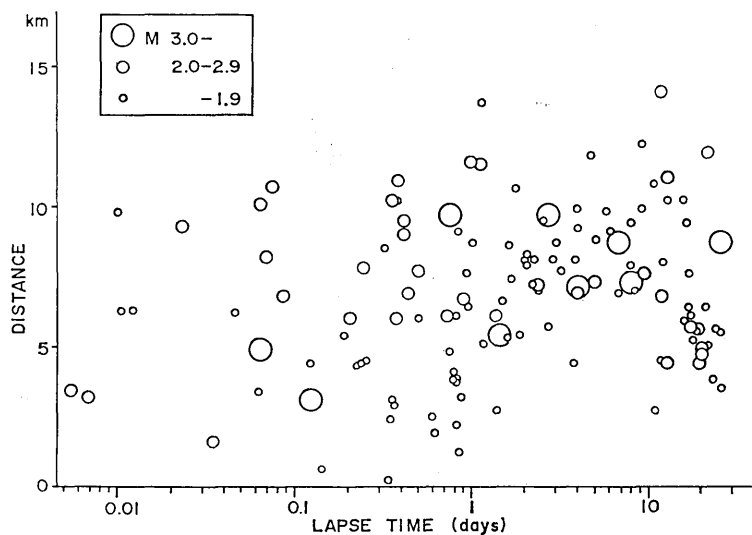


Fig. 7. The plot of the distances between the aftershocks and the main shock against the lapse time.

where t indicates the lapse time after the main shock, and n_1 , h are certain constants. For the present time series, $n_1=1,120$ and $h=0.71$ (Fig. 6). The value of h is considered to be around 1.0 or slightly larger in ordinary aftershock sequences, as examined by Mogi (1962). Some studies, however, indicate that h values are considerably smaller at certain swarm areas (Ohtake *et al.*, 1967; Ohtake, 1970).

It is sometimes found that aftershock areas spread gradually with time until they form the whole areas (for instance, Mogi, 1968; Watanabe and Kuroiso, 1969). The spreading process is somewhat complicated in our case. Fig. 7 shows a remarkable expansion of the aftershock region in the seven hours following the occurrence of the largest aftershock, that is three hours (0.13 day) after the main shock. Before this event, however, the foci seem to be distributed in a wide range of focal distances from the main shock. A considerable number of the aftershocks are found near the main shock in the first 24 hours, but they almost completely disappear afterwards, especially within five kilometers from the main event.

7. Frequency distribution of the magnitudes.

The empirical formula:

$$M = -4.57 + 3.63 \log \tau,$$

is used to estimate the local magnitude of the earthquakes, where τ is the total duration time in seconds on the high sensitivity records at

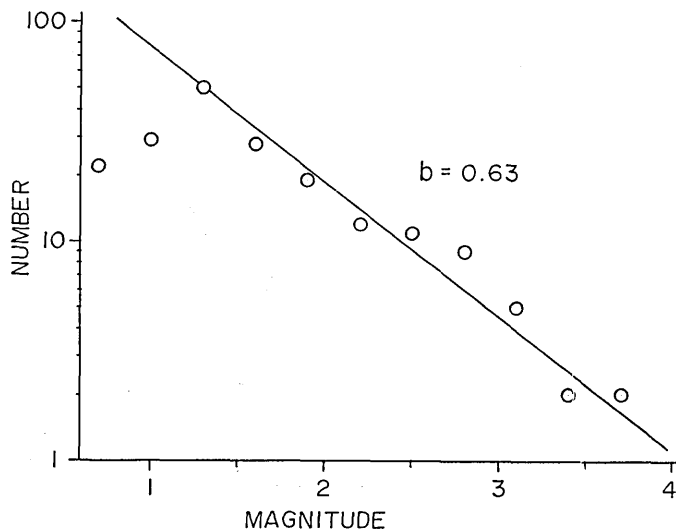


Fig. 8. The magnitude-frequency distribution of the aftershocks.

Ohmine. As shown in Fig. 8, logarithm of the number keeps almost linear relation against the magnitudes, and 0.63 is obtained for Gutenberg-Richter's b value by Utsu's (1965) method. Ishimoto-Iida's coefficient, m , is estimated to be 1.71 at Ohmine in a wide amplitude range of 60 db. Correspondence of both values is fairly good. These values are a little smaller than those obtained by other investigations on Matsushiro earthquakes (for instance, JMA, 1968).

8. Foreshocks.

A notable foreshock occurred 12.7 seconds prior to the main shock. Its magnitude was 3.4 (Hokushin), and was almost comparable with the largest aftershock, whose magnitude was 3.7 (Hokushin). This foreshock is located on the seismic plane of the larger aftershocks. Except for this one, any foreshocks with magnitude larger than 1.2 could not be found within three days just before the main event. It is, however, a fact that ultra microearthquakes had begun to occur two hours before the coming event. Such shocks were so small that only the nearest station, Kami-muroga, could just detect them. Their time series is illustrated in Fig. 9.

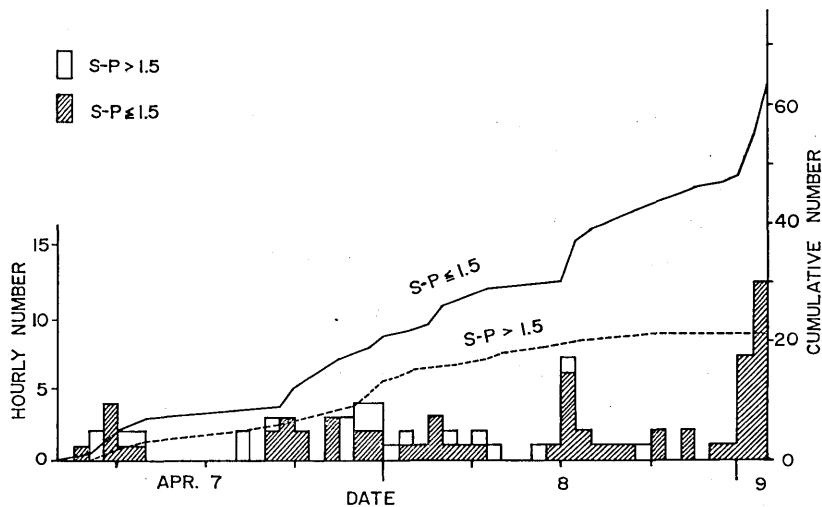


Fig. 9. The time series of the microearthquakes observed at Kami-muroga just before the main shock.

9. Energy release.

The epicenters of the Matsushiro earthquakes are not distributed uniformly in their swarm area. Several numbers of highly active groups

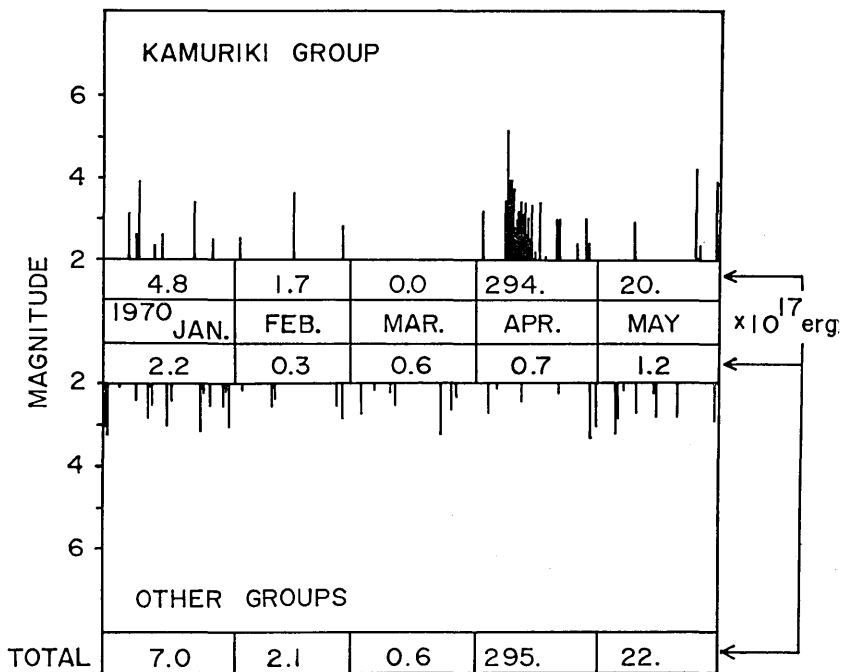


Fig. 10. The energy release from the swarm area of the Matsushiro earthquakes.

are recognized through the swarm activity, and between them lie the regions with lower activity (Hamada, 1968). The present event occurred just in one of such active groups, situated on the southern foot of Mt. Kamuriki. We call it tentatively "Kamuriki group".

On Fig. 10 is estimated the energy release from the Kamuriki group compared with that from the other regions of the swarm area. Estimation of the wave energy is based on the formula:

$$\log E = 11.8 + 1.5M.$$

The monthly energy release from the whole swarm area was 16.8×10^{17} ergs on average through 1969, accompanying no earthquakes whose magnitude exceeds 4.5. Compared with this value, the released energy is substantially less in the three months preceding the earthquake on April 9. The activity level seems to go down through these three months, especially at the Kamuriki group. In March no shocks were registered with magnitude larger than 2.0 in this group. It is noteworthy that the energy release from the other active groups is nearly constant through the five months examined. The effect of the big event was restricted only to the Kamuriki group, and it never disturbed the seismicity of the other groups.

10. Discussion.

The feature of the hypocentral distribution.

The following characteristics are ascertained concerning the hypocentral distribution. (1) Aftershocks are distributed in a rectangular region placing the main shock close to one end of it. (2) The foreshock and the larger aftershocks show an arrangement of a plate, and the smaller ones are mainly clustered by the upper side of it. (3) The size of the active region satisfies some empirical relations resulting from studies on larger earthquakes. These facts would insist upon some common characteristics with large-scale earthquakes, in the process of the fracture forming and the pattern of the residual stress field after the main shocks.

The fault plane of the main shock.

No fault trace was observed around the focal region. The plot of the aftershocks (Fig. 5), however, suggests that the top of the fault plane may reach five kilometers beneath the ground surface. The strike of the seismic plane of the larger aftershocks almost coincides with one of the nodal lines of the main shock. If this seismic plane is considered to be a projection of the fault plane accompanying the main shock, the process of fracturing can be described as follows: a left-lateral dislocation ran aslant upwards for ten kilometers from depths of 14 km to 5 km, where the width of the fault plane was two kilometers.

The independent behavior of the active groups.

The largest magnitude of the Matsushiro earthquakes was 5.4 through these five years, and no shocks exceeded 5.5. About six larger earthquakes, however, are expected from the linear relation between magnitude and logarithm of frequency in the magnitude range less than 5.0 (Fig. 11). On the other hand, Dambara (1966) estimated the probable largest earthquake

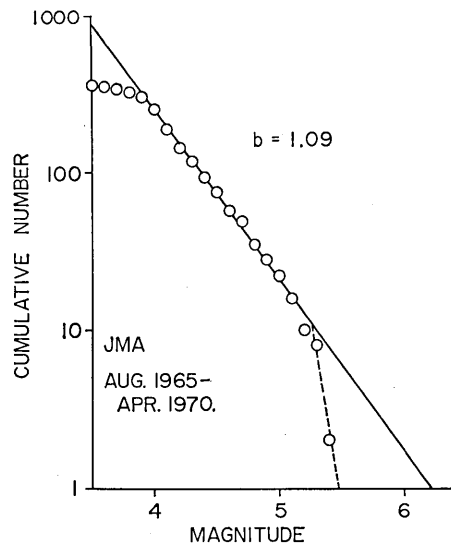


Fig. 11. The magnitude-frequency distribution of the Matsushiro earthquakes, based on the data of JMA.

to be 6.6 from the area of the crustal deformation around Matsushiro. He called our attention to the fact that the corresponding energy release agrees well with the cumulative wave energy emitted by the Matsushiro earthquakes, although no physical explanation was given. It is an apparently curious lack of shocks with magnitude larger than 5.5, so far as the whole swarm area is considered to be a single active unit. Our investigations, on the contrary, suggest the independent nature of each active group in the swarm area (section 9). If the swarm area is divided into several blocks and each one behaves independently under the effect of a regional stress field, the lack of larger shocks is naturally explained. Actually, some groups were very active at the early stages, and some others appeared and took active parts at the later stages, when certain groups were already in the period of decadance.

The fractured condition of the medium.

This activity showed a foreshock—main shock—aftershock type, but some properties of the sequence indicate a somewhat swarmlike tendency. First, decaying of the aftershock frequency is slow as mentioned in section 6. Second, the magnitude of the largest aftershock is as high as 3.7, which corresponds to a 5.9 main shock after Utsu's (1961) empirical relation:

$$\overline{M_0 - M_1} = 4.9 - 0.47 M_0, \quad (6 \leq M_0 < 8 \frac{1}{2}),$$

where M_0 and M_1 are the magnitudes of the main shock and the largest aftershock, and the left side indicates the mean value of the magnitude difference. These facts may be reflecting the fractured condition of the medium.

Acknowledgement

The author wishes to express his sincere thanks to Mr. M. Katsumata of the Seismological Section of JMA for kindly providing the unpublished data of JMA stations. The travel times were computed by Dr. S. Kubota with his own program. A part of the records was read by Mr. K. Kimura and Mr. M. Kobayashi of the Hokushin Observatory, for whose helpful co-operation the author's thanks are due. He is also very grateful to Prof. S. Miyamura and Prof. H. Kanamori for their valuable suggestions.

References

- ASANO, S., S. KUBOTA, H. OKADA, M. NOGOSHI, H. SUZUKI, K. ICHIKAWA, and H. WATANABE, 1969, Explosion seismic studies of the Matsushiro earthquake swarm area, *Jour. Phys. Earth*, **17**, 77-90.

- DAMBARA, T., 1966, Vertical movements of the earth's crust in relation to the Matsushiro earthquake (in Japanese), *Jour. Geod. Soc. Japan*, **12**, 18-45.
- HAMADA, K., 1968, Ultra micro-earthquakes in the area around Matsushiro, *Bull. Earthq. Res. Inst.*, **46**, 271-318.
- ICHIKAWA, M., 1969, Matsushiro earthquake swarm, *Geophys. Mag.*, **34**, 307-331.
- IIDA, K., 1963, A relation of earthquake energy to tsunami energy and the estimation of the vertical displacement in a tsunami source, *Jour. Earth Sci. Nagoya Univ.*, **11**, 49-67.
- JAPAN METEOROLOGICAL AGENCY, 1968, Report on the Matsushiro earthquake swarm, August 1965-December 1967 (in Japanese), *Tech. Report JMA*, **62**, 52-57, 65-67.
- MOGI, K., 1962, On the time distribution of aftershocks accompanying the recent major earthquakes in and near Japan, *Bull. Earthq. Res. Inst.*, **40**, 107-124.
- MOGI, K., 1968, Development of aftershock areas of great earthquakes, *Bull. Earthq. Res. Inst.*, **46**, 175-203.
- OHTAKE, M., H. CHIBA, and T. HAGIWARA, 1967, Ultra micro-earthquake activity at the southwestern border of the area of Matsushiro earthquakes. Part 1, *Bull. Earthq. Res. Inst.*, **45**, 861-886.
- OHTAKE, M., 1970, On an earthquake activity that occurred near Kamikochi (in Japanese), *Bull. Earthq. Res. Inst.*, **48**, 65-71.
- UTSU, T., and A. SEKI, 1955, A relation between the area of after-shock region and the energy of main-shock (in Japanese), *Zisin, Jour. Seism. Soc. Japan*, [ii], **7**, 233-240.
- UTSU, T., 1961, A statistical study on the occurrence of aftershocks, *Geophys. Mag.*, **30**, 521-605.
- UTSU, T., 1965, A method for determining the value of b in a formula $\log n = a - bM$ showing the magnitude-frequency relation for earthquakes (in Japanese), *Geophys. Bull. Hokkaido Univ.*, **13**, 99-103.
- WATANABE, H., and A. KUROISO, 1969, Seismic activity in the northern part of the Kinki district and related problems (I), *Spec. Contr. Geophys. Inst. Kyoto Univ.*, **9**, 123-136.

56. 中規模地震前後の地震活動の微細構造

地震研究所 大竹政和

1970年4月9日、松代付近に発生した $M=5.0$ (気象庁) の中規模地震について、その前後の地震活動の微細構造を調べた。余震域はわずか 18 km^2 にすぎないが、信頼度の高い観測と解析によって次のような特徴ある余震空間分布を見出すことができた。

(1) 比較的大きい余震及び前震は、長さ 10 km 、巾 2 km の傾斜した「余震面」に添って排列する傾向を示す。より小さい余震はこの面より上方に分布するものが圧倒的に多いが、深さ 9 km 以浅では下方にも多数の震源が分布する。(2) 主震は余震面の最深端に位置する。この付近では余震活動が相対的に不活である。(3) 余震面の走行は、主震の初動押引分布の一方の節線と概ね一致する。

この余震面を主震に伴う破壊面とみなすことが許されるならば、左横ずれのくいちがいが地下 14 km から斜め上方に向かって約 10 km 進んだことになる。

此度の地震は、松代地震群発域内の顕著な活動群のひとつに発生した。しかし地震発生の直前2~3ヶ月の間特にこの活動群は異常に静穏であった。余震はこの活動群の範囲内に限られ、主震の前後数ヶ月を通じて、他の活動群からのエネルギー放出水準は何らの影響も受けなかった。松代地震の群発域は、このように相互に独立した数個の活動ブロックの集合体として理解するべきではなからうか、全群発域を単一の「地震体積」とするような $M6$ 規模の地震が現在まで発生していないという事実は、松代付近の地殻浅部がいくつかのブロックに分割されていることを示唆している。